

Observation of the inward propagation of spontaneous toroidal flow from the plasma boundary in LHD

Cite as: Phys. Plasmas **23**, 102309 (2016); <https://doi.org/10.1063/1.4965908>

Submitted: 12 September 2016 • Accepted: 10 October 2016 • Published Online: 25 October 2016

 K. Kamiya, K. Ida, K. Itoh, et al.



View Online



Export Citation



CrossMark

ARTICLES YOU MAY BE INTERESTED IN

[Novel analysis technique for measuring edge density fluctuation profiles with reflectometry in the Large Helical Device](#)

Review of Scientific Instruments **88**, 073509 (2017); <https://doi.org/10.1063/1.4993437>

[Structure formation in parallel ion flow and density profiles by cross-ferroic turbulent transport in linear magnetized plasma](#)

Physics of Plasmas **23**, 102311 (2016); <https://doi.org/10.1063/1.4965915>

[Observation of the ECH effect on the impurity accumulation in the LHD](#)

Physics of Plasmas **24**, 056118 (2017); <https://doi.org/10.1063/1.4983626>

Physics of Plasmas

Papers from 62nd Annual Meeting of the
APS Division of Plasma Physics

Read now!



Observation of the inward propagation of spontaneous toroidal flow from the plasma boundary in LHD

K. Kamiya,^{1,a)} K. Ida,² K. Itoh,^{2,3} S.-I. Itoh,^{3,4} M. Yoshinuma,² M. Yokoyama,² S. Kubo,² H. Tsuchiya,² N. Tamura,² S. Masuzaki,² C. Suzuki,² T. Akiyama,² and LHD Experiment Group

¹National Institutes for Quantum and Radiological Science and Technology (QST), Naka, Ibaraki-ken 311-0193, Japan

²National Institute for Fusion Science (NIFS), Toki, Gifu 509-5292, Japan

³Itoh Research Center for Plasma Turbulence, Kyushu University, Kasuga 816-8580, Japan

⁴Research Institute for Applied Mechanics, Kyushu University, Kasuga 816-8580, Japan

(Received 12 September 2016; accepted 10 October 2016; published online 25 October 2016)

Spontaneous generation of toroidal flow from the separatrix and its inward radial propagation in association with the change in the electron temperature gradient have been observed near the plasma boundary in the modulated electron cyclotron heating (MECH) experiment in the Large Helical Device. The observations presented in this paper provide strongly the supports of the hypothesis for the conversion of the poloidal flow to the toroidal one at the plasma peripheral region, exhibiting a clear delay response on MECH in the time derivation of the toroidal flow ($\dot{V}_\phi \equiv \partial V_\phi / \partial t$) to the poloidal one ($\dot{V}_\theta \equiv \partial V_\theta / \partial t$) at a normalized radius of $\rho \approx 0.97$. The ratio of order unity for $|\dot{V}_\phi / \dot{V}_\theta|$ during a conversion phase from poloidal flow into toroidal one is consistent with that predicted by a quasi-stationary theoretical model based on the turbulent instability, regardless of its sign and spatial structure. The present work demonstrates a new dynamic response in the plasma momentum transport and represents a significant confirmation of its non-local nature. *Published by AIP Publishing.* [<http://dx.doi.org/10.1063/1.4965908>]

I. INTRODUCTION

In recent years, understanding the origin of the intrinsic rotation of a confined plasma and the physical meaning of the off-diagonal term of the toroidal angular momentum transport equation has attracted considerable attention, since there is strong coupling between the core and edge transport in toroidal fusion devices.^{1,2} Here we use the words “intrinsic rotation” to denote the plasma flow which is not driven by external torque nor by local diffusive process. Furthermore, it is widely recognized that plasma flow and its shear significantly contribute towards achieving higher plasma confinement along with higher system stability.

Plasma flow is usually provided by the external momentum input from neutral-beam injection (NBI) in current-generation devices. This type of external plasma control technique may find limited applications in next-generation devices due to larger machine sizes, higher densities, and beam current limitations.³ On the other hand, the phenomenon of spontaneous or intrinsic rotation in the plasma core region is observed in almost all toroidal devices, and momentum transport bifurcations are observed even in torque-free plasmas,^{4–6} thereby suggesting that the change of plasma flow is initiated at the edge and builds inward (and hence, there is an important role of edge flow affecting the intrinsic core flow as seen in the recent experimental results).

Therefore, an understanding of the driving mechanism of the intrinsic plasma flow at the edge is important towards

understanding the spontaneous generation of the plasma flow at the plasma core region in torque-free plasmas. Furthermore, the importance of scrape-off layer (SOL) flows on rotation inside the Last Closed Flux Surface (LCFS) has been discussed in detail in Ref. 7, in which plasma profiles and flows in the low- and high-field side scrape-off-layer (SOL) regions in Alcator C-Mod are found to be remarkably sensitive to magnetic separatrix topologies (upper-, lower-, and double-null) and to impose topology-dependent flow boundary conditions on the confined plasma.

The results presented here show a non-local nature for the momentum transport and provide experimental results for the test of the theory on the intrinsic rotation driven by plasma turbulences.

II. EXPERIMENTAL SETUP

The Large Helical Device (LHD) has been equipped with three 77 GHz gyrotrons with the power of ≥ 1 MW at the pulse width of 5 s. They are capable of power modulation with duty cycles of up to 100 Hz. In this letter, we focus on the fast plasma flow dynamics in the edge LHD L-mode during the modulated electron cyclotron heating (termed “MECH”) experiment at low plasma densities. In the experiment, power deposition is set to the normalized radius of $\rho_{ECH} \approx 0.85$, and the magnetic field strength and plasma configuration are adjusted as follows: the toroidal magnetic field on the vacuum magnetic axis is set to $B_T = 1.75$ T (clockwise as viewed from the top of the torus), and the plasma configuration is set to the vacuum magnetic axis position of $R_{\text{AXIS}} = 3.53$ m with the helical pitch parameter

^{a)}Author to whom correspondence should be addressed. Electronic mail: kamiya.kensaku@jaea.go.jp

being $\gamma = 1.254$. Here, γ is defined as $\gamma \equiv m_a c / (\ell R_c)$, where m , ℓ , a_c , and R_c denote the toroidal pitch number, poloidal pitch number, minor radius, and major radius of the helical coil, respectively.

The key diagnostic used for measuring the plasma flow profiles was Charge-eXchange recombination Spectroscopy (CXS) with high temporal (200 Hz) and spatial (1–2 cm) resolution, having the viability of determination of the radial electric field structure by means of the radial force balance equation as follows: $E_r = \frac{\nabla p_i}{Z_i e n_i} - V_{\theta j} B_\phi + V_{\phi j} B_\theta$. Where Z_j is the ion charge, n_j is the ion density, e is the elementary charge, $\nabla p_j = n_j T_j$ is the ion pressure with T_j being the ion temperature, $V_{\theta j}$ and $V_{\phi j}$ are the ion poloidal and toroidal rotation velocities, respectively, and B_ϕ and B_θ are the poloidal and toroidal magnetic fields, respectively. The measured profile data in real coordinates (R , Z) are mapped to an effective minor radius, r_{eff} , by using the best-fit Variational Moments Equilibrium Code (VMEC)⁸ and the location of the separatrix ($a_{\text{eff}}^{\text{LCFS}}$) at which the spatial derivative in the E_r structure (∇E_r) exhibited a local maximum value was determined by using CXS diagnostics.⁹

To investigate the response of the edge plasma to electron heat pulse propagation, we performed the MECH experiment with a duty cycle of 40 Hz. With regard to determining the response of the plasma flows due to MECH, improvements have been made in obtaining statistics in assessing the temporal behavior of the measurements by mapping multiple, reproducible MECH cycles onto a single time basis, which is defined by the time of the measurement relative to the MECH (the so-called “conditional averaging method”).

III. RESULTS

The relative perturbations to the electron temperature, T_e , its radial derivative, ∇T_e , and radial electric field, E_r , at the plasma edge region, in conjunction with the velocity changes near the ECH deposition layer as has been observed in tokamaks (see, e.g., the review Ref. 2), are shown in Fig. 1 via comparison between the pre- and post-MECH stages. The perturbation for T_e becomes large close to the separatrix (Fig. 1(a)). It is important that the magnitude of electron temperature gradient inside ECH deposition layer ($\rho \leq \rho_{\text{ECH}} \approx 0.85$) decreases by applying ECH, while the magnitude of electron temperature gradient outside ECH deposition layer ($\rho \geq \rho_{\text{ECH}} \approx 0.85$) increases after ECH-on (Fig. 1(b)). This simultaneous increase and decrease of temperature gradient (the code-edge coupling) is considered to be one of the non-locality phenomena of heat transport.¹⁰ As illustrated in Fig. 1(c), a change in the T_e (and/or collisionality) brings a corresponding change in the E_r (and/or $E \times B$ flow) on the helical system,¹¹ exhibiting a quantitative difference with the neoclassical model calculation based on the ambipolar condition inside the separatrix.¹² Above all, the E_r structure had an isolated “hill” structure around $\rho \approx 0.94$ – 0.96 , at which the poloidal flow component is a dominant contributor to the total E_r in the carbon impurity ion radial force balance equation. The most interesting point is that the response of the V_ϕ structures (Fig. 1(d)) on the MECH exhibit a non-diffusive nature as that seen in the electron heat transport (i.e., the gradient in

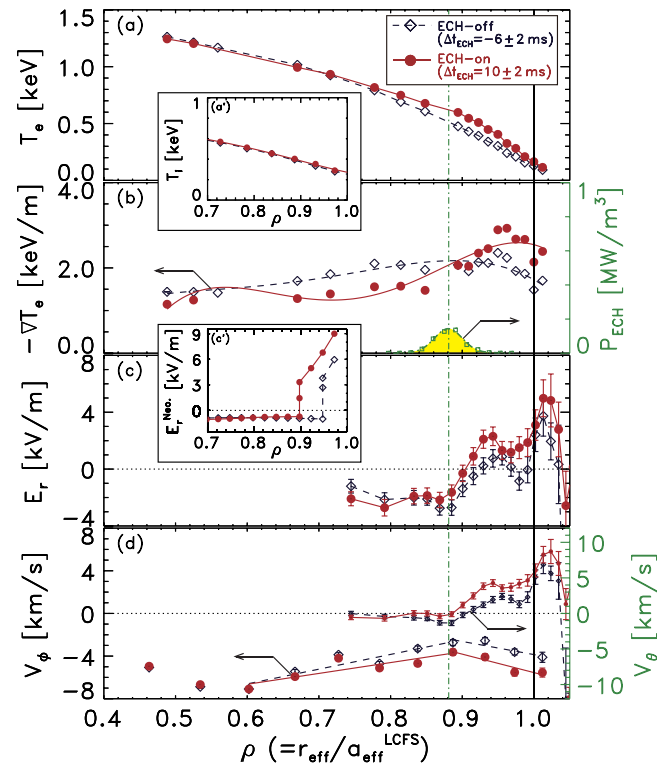


FIG. 1. Measured profiles of (a) electron temperature T_e , (b) radial derivative of electron temperature ∇T_e and ECH power deposition profile from a ray tracing calculation P_{ECH} , (c) radial electric field E_r , and (d) toroidal flow V_ϕ and poloidal flow V_θ , comparing before (blue diamonds) and after (red circles) Modulation ECH power application. The radial coordinate is normalized by the effective minor radius $\rho \equiv r_{\text{eff}} / a_{\text{eff}}^{\text{LCFS}}$. Profiles for measured ion temperature and neoclassical calculation of the radial electric field are also shown in (a') and (c').

the plasma flow inside ECH deposition layer decreases by applying ECH, while it increases outside ECH deposition layer after ECH-on). It should be noted that the change in the ion temperature and its gradient in association with the ECH-on/off is negligibly small in comparison with that of electron temperature, since the direct input power to the bulk ion from the ECH is less significant than that of electron.

Upon application of ECH (Fig. 2(a)), the line-averaged electron density decreases up to $\sim 5\%$ in the edge chord passing through $\rho \gg 0.85$, and hence we will discuss only the change in the plasma flow (not for momentum itself) later. Together with a small decrease in the edge density, we observed an increase in the particle flux to the divertor, as inferred from the change in the ion saturation current, I_s , and/or H_α emission (Fig. 2(b)). This observation suggests that the increase of the turbulence-driven radial flux of electron energy at the boundary region during ECH-on phase. In addition, the electron heat pulse appears to propagate across to the separatrix, as inferred from the temporal evolutions in T_e around the plasma boundary region across the separatrix (Fig. 2(c)).

As illustrated in Figs. 2(d) and 2(e), we observed a clear response to the MECH on both V_ϕ and V_θ profiles at the plasma peripheral region in association with the change in the edge ∇T_e . This observation makes it possible to investigate the impact on the driving mechanism underlying the edge toroidal/poloidal flows even in the electron heating

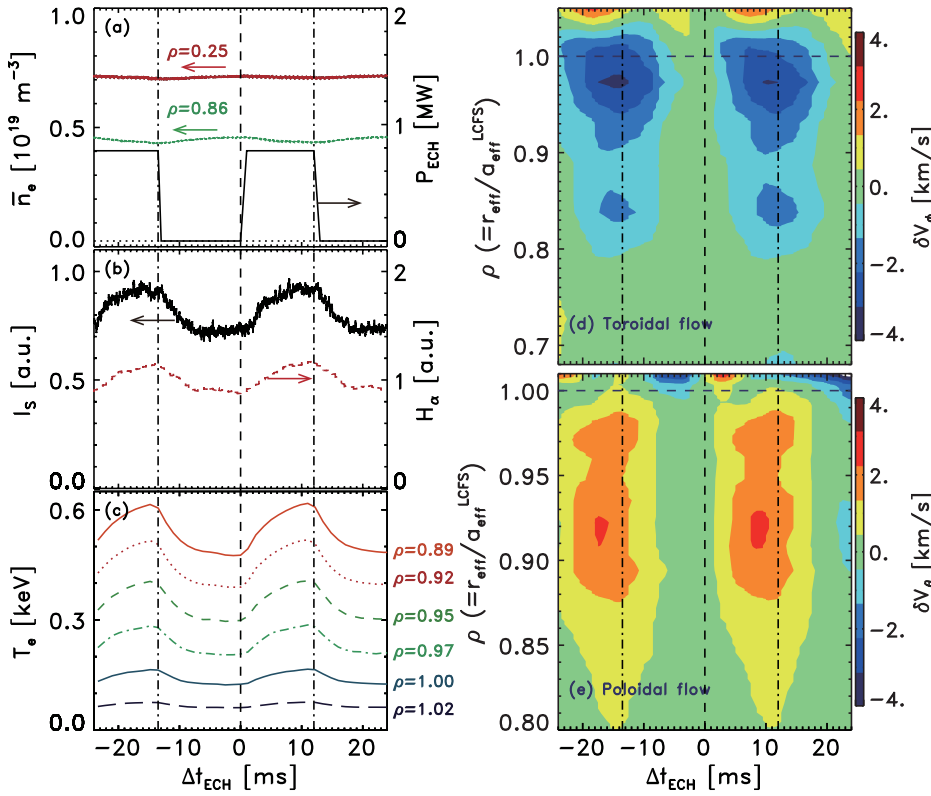


FIG. 2. Temporal evolution of (a) line-averaged electron density measured by the vertical array passing through points corresponding to the normalized effective minor radius $\rho=0.25$ and 0.85 and ECH power, (b) ion saturation current and H_α emission at the divertor, (c) edge electron temperature profiles T_e for the normalized effective minor radii ranging from $\rho=0.89$ to 1.02 , and contour plots for the relative changes in the edge (d) toroidal and (e) poloidal flow profiles $\delta V_{\phi,\theta} \equiv V_{\phi,\theta}(\rho, \Delta t) - V_{\phi,\theta}(\rho, \Delta t=0)$ during a MECH cycle constructed by organizing the data with respect to the measurement time relative to the closest MECH-on $\Delta t \equiv t - t_{\text{MECH-on}}$.

experiment without an external toroidal momentum input. Looking at Fig. 2(d), the spontaneous radial propagation in the toroidal flow from the plasma boundary could be seen more clearly at the plasma peripheral region outside the ECH power deposition ($\rho \geq \rho_{ECH} \approx 0.85$), while both poloidal/toroidal plasma flows remain the same within the errors of the measurement at the plasma core region inside the ECH power deposition ($\rho \leq \rho_{ECH} \approx 0.85$). This observation suggests that the plasma flow generation at the plasma peripheral region in the toroidal magnetic confinement system is not likely to be able to explain by the diffusive transport model as well as the plasma heat transport (cf. electron temperature gradient as shown in Fig. 1(b)). It should be noted that the change in V_ϕ near the plasma boundary region according to the electron heat-pulse propagation is in the direction opposite to the increasing rotational transform direction (corresponding to the negative E_r value), while the change in V_θ is in the ion diamagnetic direction (corresponding to the positive E_r value), rebounding out of phase with each other.¹³

At the onset of the ECH-on/off phases, the temporal response for the change in the time derivation of the poloidal plasma flow, $\dot{V}_\theta \equiv \partial V_\theta / \partial t$, seems to proceed from that of the toroidal one, $\dot{V}_\phi \equiv \partial V_\phi / \partial t$. This tendency becomes more clear when we compare the information regarding the change in the poloidal and toroidal momentum balance during the MECH process, garnering up the responses of the poloidal and toroidal viewing CXS systems. As a result, we observed hysteresis only in the relationship between the ∇T_e and V_ϕ (not for V_θ) at $\rho \sim 0.97$ (Figs. 3(a) and 3(b)), at which the change in the toroidal flow due to the MECH was followed by the poloidal one (Fig. 3(c)). This experimental data

reveals new phenomena of the conversion of poloidal flow into toroidal one near the plasma boundary region.

Effect of the plasma flow conversion from poloidal direction into toroidal one is predicted by a quasi-stationary theoretical model based on the turbulent instability in a toroidal/poloidal doubly bounded magnetic confinement system.¹⁴ It is associated with one general mechanism of an enhancement in the drift-wave turbulence due to the change in the electron temperature gradient. Once the poloidal flow generated by the plasma turbulence (as is explained in Ref. 14), it could be converted into the toroidal flow by phase space structures in trapped ion resonance driven turbulence as a candidate for the driving force in the toroidal flow.¹⁵ As discussed in Ref. 15, the conversion factor, $M_{\phi \leftarrow \theta}^{gran}$, could be determined by the relationship between the time derivative of the toroidal and poloidal flows (i.e., $\dot{V}_\phi = M_{\phi \leftarrow \theta}^{gran} \times \dot{V}_\theta$). It should be noted that the radial electric field almost always

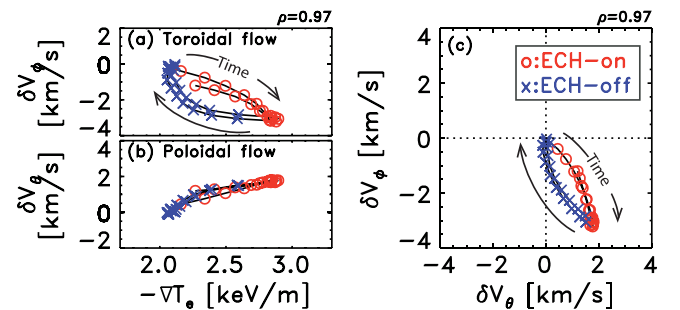


FIG. 3. Lissajous figures of the relative changes in (a) toroidal flow δV_ϕ and (b) poloidal flow δV_θ versus electron temperature gradient ∇T_e at a normalized effective minor radius $\rho=0.97$. Relationship between toroidal flow and poloidal flow at $\rho=0.97$ is also shown in (c).

play an important role for the neo-classical transport (turbulent transport as well), especially for helical plasmas. Therefore, it is possible that the rotational motion of ions is induced being associated with the electron temperature gradient via a strong coupling between the electron heat transport and radial electric field. If so (as seen in Fig. 3(b), partially), it is possible that the $E \times B$ rotational motion of ions could appear towards the poloidal direction because of damping of the plasma toroidal velocity owing to parallel viscosity as discussed in Ref. 2. These mutual couplings should be concluded, after examining dependencies of the present observation on various discharges with different global plasma parameters.

Looking at Fig. 4, the ratio of the time derivation of the toroidal flow to the poloidal one ($\xi \equiv -\dot{V}_\phi/\dot{V}_\theta$) at $\rho \sim 0.97$ is order of unity during a conversion phase from poloidal plasma flow into toroidal one as that predicted by the theoretical model, regardless of its sign and spatial structure (this will be discussed later).

It should be noted that the observed spatial structure for the toroidal flow in the plasma peripheral region on LHD seems to be different from the poloidal one (and/or $E \times B$ flow) and the direction of toroidal flow is in the counter-direction in the plasma with positive E_r as shown in Figs. 1(c) and 1(d). This is in contrast to the observation of Pfirsch-Schlüter flow in the H-mode edge region on tokamaks.¹⁶ Furthermore, the time-scale of the spontaneous toroidal flow generation in this experiment is much longer than the relaxation time-scale between the force and driven plasma flow expected by the neo-classical model as the inverse of the parallel viscosity coefficient, $\mu_{\parallel}^{-1} \approx 50 \mu\text{s}$.¹⁷ In fact, previous studies on JFT-2M had shown that the toroidal flow could be generated by the density and/or ion temperature gradient as a non-diffusive term in the transport matrix.¹⁸ The new finding in this study is the observation of the spontaneous toroidal flow generation by the electron temperature gradient.

IV. DISCUSSION

It is interesting to carry the speculation on what happens during the electron heat-pulse propagation from core to edge region. The spatial structure of the plasma flow conversion (as evaluated by the $\xi \equiv -\dot{V}_\phi/\dot{V}_\theta$ is illustrated in Fig. 4) had a local maximum value of order unity at $\rho \sim 0.97$ (corresponding to the distance from the separatrix is about a few 10 times of the ion poloidal Larmor radius, ρ_{θ_i}). On the other hand, the ξ value became smaller at the separatrix. Since the toroidal plasma flow is more parallel to the magnetic field line than that of the poloidal one, the former could be affected by the momentum losses as a result of an incompletely nesting magnetic field lines. And hence, the conversion process from poloidal to toroidal flow should be damped (i.e., $\xi \rightarrow 0$) at the separatrix. Moreover, one can find that the ξ value also became smaller at the plasma core region inside the ECH power deposition (e.g., $\rho \leq 0.85$), where the plasma turbulence may be smaller than that at the separatrix (there should be a different nature between the core and edge regions, at least).

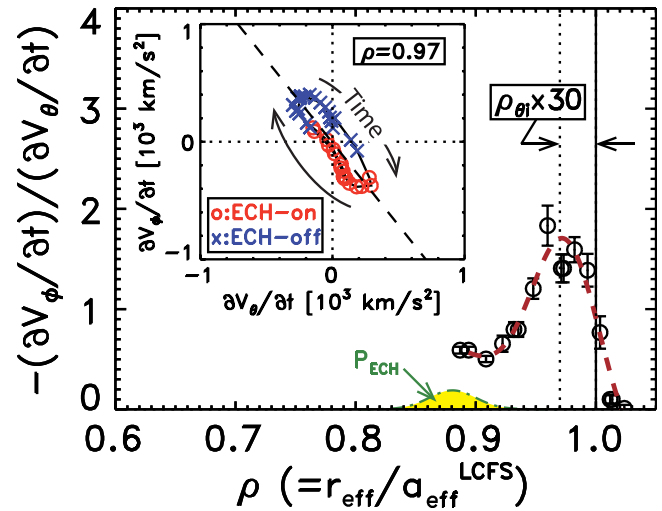


FIG. 4. Measured profile of the ratio of the time derivation of the toroidal flow to the poloidal one ($\xi \equiv -\dot{V}_\phi/\dot{V}_\theta$). The local peak that appears at a distance from the separatrix is about a few 10 times of the ion poloidal Larmor radius, ρ_{θ_i} (corresponding normalized effective radius of $\rho \sim 0.97$). Lissajous figures of time derivative of toroidal flow, $\partial V_\phi/\partial t$, versus poloidal one, $\partial V_\theta/\partial t$, at $\rho = 0.97$ is also shown.

We also point out the in-out asymmetry of propagation of perturbations (which are driven by MECH) with respect to the heating position. Induced changes of T_e (∇T_e) and V_ϕ show much smaller penetrations into core in comparison to the expectation of diffusive models. This is in contrast to the fact that the edge intrinsic rotation is roughly proportional to the H-mode pedestal temperature gradient in steady state.¹⁹ On the other hand, we found that the dynamic characteristics of intrinsic plasma flow generation could be quite different from that expected from the parameter dependence in steady state (cf. the change in plasma stored energy normalized to plasma current, $\Delta V_\phi \propto \Delta W_P/I_P^2$), which is an important knowledge towards predicting the dynamics of intrinsic plasma rotation in future fusion devices. This result seems not to be self-evident when only referring to the previous knowledge of the plasma core region. Recently, a possible working hypothesis to explain this observation has been developed, i.e., the coupling between fluctuations and external heating can work as a new source that drives the fluctuations and turbulence as discussed in Refs. 20 and 21. This issue of deviation from diffusive response will be discussed in detail in future reports.

V. SUMMARY AND FUTURE DIRECTION

With regard to determining the response of the edge plasma flows due to the electron heat-pulse, we performed the modulated electron cyclotron heating (MECH) experiment on LHD. Here we reported that a significant improvement in statistics had been made in assessing the temporal behavior of the measurements by means of conditional averaging method. This advancement resulted in a new finding of spontaneous generation of toroidal flow from the separatrix and its inward radial propagation in association with the change in the electron temperature gradient near the plasma boundary. The observation supports the hypothesis for the

conversion of the poloidal flow to the toroidal one at the plasma peripheral region.

There has been an increasing recognition in recent years concerning the relative importance of the plasma boundary condition for a diverted fusion device, in which there is a strong relationship between the core and edge regions in terms of plasma transport. As discussed in Ref. 3, plasma rotation is usually provided by the external momentum input from neutral beam injection in the current generation of tokamaks. However, this may not provide the necessary rotation in future reactor-grade devices due to the large machine sizes, high densities, and the limitations of beam current. For the resistive wall mode (RWM) stabilization in certain ITER operational scenarios, it remains an open question whether the required level of rotation (e.g., an Alfvén Mach number $MA \sim 0.02$) will be generated from neutral beams alone, and hence the intrinsic (spontaneous) rotation without external momentum input is expected to provide the necessary velocity. Nevertheless, the mechanism of driving intrinsic rotation is not yet well understood. In order to anticipate the level of rotation expected in ITER and other reactor devices, a database of observations on several contemporary machines (including helicals) has been constructed. It should be noted that a non-axisymmetric geometry may be more commonly generated in nature, this paper reports the essential advancement of plasma physics. The study in this article has also substantial importance in application of thermonuclear fusion research, because the symmetry-breaking perturbation coils have been more and more widely applied to many tokamaks.²² Above all, the mechanism related to the turbulence driven one, as presented in this paper, should have a relative importance for a common physics understanding in the torus plasmas. In particular, studies on the momentum transport during the inter-ELM (edge localized mode) period after the loss of Er shear at the ELM event in terms of the neoclassical and/or turbulent transport will become an issue in the future.

ACKNOWLEDGMENTS

We thank Dr. Y. Kosuga and Dr. N. Kasuya for useful discussions. This work was supported by NIFS/NINS under the NIFS Collaborative Research Program (NIFS10KLHH314 and NIFS10KLPH006) and a Grant-in-Aid for Scientific Research of JSPS, Japan (15K06657, 15H02155, and 16H02442).

¹P. H. Diamond, C. J. McDevitt, Ö. D. Gürcan, T. S. Hahm, W. X. Wang, E. S. Yoon, I. Holod, Z. Lin, V. Naulin, and R. Singh, *Nucl. Fusion* **49**, 045002 (2009).

²K. Ida and J. E. Rice, *Nucl. Fusion* **54**, 045001 (2014).

³J. E. Rice, A. Ince-Cushman, J. S. deGrassie, L.-G. Eriksson, Y. Sakamoto, A. Scarabosio, A. Bortolon, K. H. Burrell, B. P. Duval, C. Fenzi-Bonizze, M. J. Greenwald, R. J. Groebner, G. T. Hoang, Y. Koide, E. S. Marmor, A. Pochelon, and Y. Podpaly, *Nucl. Fusion* **47**, 1618–1624 (2007).

⁴J. E. Rice, A. C. Ince-Cushman, M. L. Reinke, Y. Podpaly, M. J. Greenwald, B. LaBombard, and E. S. Marmor, *Plasma Phys. Controlled Fusion* **50**, 124042 (2008).

⁵A. Bortolon, B. P. Duval, A. Pochelon, and A. Scarabosio, *Phys. Rev. Lett.* **97**, 235003 (2006).

⁶K. Ida, Y. Sakamoto, H. Takenaga, N. Oyama, K. Itoh, M. Yoshinuma, S. Inagaki, T. Kobuchi, A. Isayama, T. Suzuki, T. Fujita, G. Matsunaga, Y. Koide, M. Yoshida, S. Ide, Y. Kamada, and JT-60 Team, *Phys. Rev. Lett.* **111**, 055001 (2013).

⁷B. LaBombard, J. E. Rice, A. E. Hubbard, J. W. Hughes, M. Greenwald, J. Irby, Y. Lin, B. Lipschultz, E. S. Marmor, C. S. Pitcher, N. Smick, S. M. Wolfe, S. J. Wukitch, and Alcator Group, *Nucl. Fusion* **44**, 1047–1066 (2004).

⁸C. Suzuki, K. Ida, Y. Suzuki, M. Yoshida, M. Emoto, and M. Yokoyama, *Plasma Phys. Controlled Fusion* **55**, 014016 (2013).

⁹K. Kamiya, K. Ida, M. Yoshinuma, C. Suzuki, Y. Suzuki, M. Yokoyama, and LHD Experiment Group, *Nucl. Fusion* **53**, 013003 (2013).

¹⁰K. Ida, Z. Shi, H. J. Sun, S. Inagaki, K. Kamiya, J. E. Rice, N. Tamura, P. H. Diamond, G. Dif-Pradalier, X. L. Zou, K. Itoh, S. Sugita, O. D. Gürcan, T. Estrada, C. Hidalgo, T. S. Hahm, A. Field, X. T. Ding, Y. Sakamoto, S. Oldenburger, M. Yoshinuma, T. Kobayashi, M. Jiang, S. H. Hahn, Y. M. Jeon, S. H. Hong, Y. Kosuga, J. Dong, and S.-I. Itoh, *Nucl. Fusion* **55**, 013022 (2015).

¹¹K. Ida, T. Shimozuma, H. Funaba, K. Narihara, S. Kubo, S. Murakami, A. Wakasa, M. Yokoyama, Y. Takeiri, K. Y. Watanabe, K. Tanaka, M. Yoshinuma, Y. Liang, N. Ohya, and LHD Experimental Group, *Phys. Rev. Lett.* **91**, 085003 (2003).

¹²M. Yokoyama, K. Ida, H. Sanuki, K. Itoh, K. Narihara, K. Tanaka, K. Kawahata, N. Ohya, and LHD Experimental Group, *Nucl. Fusion* **42**, 143–149 (2002).

¹³K. Ida, T. Minami, Y. Yoshimura, A. Fujisawa, C. Suzuki, S. Okamura, S. Nishimura, M. Isobe, H. Iguchi, K. Itoh, S. Kado, Y. Liang, I. Nomura, M. Osakabe, C. Takahashi, K. Tanaka, and K. Matsuoka, *Phys. Rev. Lett.* **86**, 3040 (2001).

¹⁴P. H. Diamond, C. J. McDevitt, Ö. D. Gürcan, T. S. Hahm, and V. Naulin, *Phys. Plasmas* **15**, 012303 (2008).

¹⁵Y. Kosuga, S.-I. Itoh, P. H. Diamond, and K. Itoh, *Plasma Phys. Controlled Fusion* **55**, 125001 (2013).

¹⁶T. Pütterich, E. Wolfrum, R. Dux, C. F. Maggi, and ASDEX Upgrade Team, *Phys. Rev. Lett.* **102**, 025001 (2009).

¹⁷K. Ida and N. Nakajima, *Phys. Plasmas* **4**, 310–314 (1997).

¹⁸K. Ida, Y. Miura, T. Matsuda, K. Itoh, S. Hidekuma, S.-I. Itoh, and JFT-2M Group, *Phys. Rev. Lett.* **74**, 1990 (1995).

¹⁹J. E. Rice, J. W. Hughes, P. H. Diamond, Y. Kosuga, Y. A. Podpaly, M. L. Reinke, M. J. Greenwald, Ö. D. Gürcan, T. S. Hahm, A. E. Hubbard, E. S. Marmor, C. J. McDevitt, and D. G. Whyte, *Phys. Rev. Lett.* **106**, 215001 (2011).

²⁰S.-I. Itoh and K. Itoh, *Sci. Rep.* **2**, 860 (2012).

²¹S.-I. Itoh and K. Itoh, *Nucl. Fusion* **53**, 073035 (2013).

²²T. E. Evans, R. A. Moyer, K. H. Burrell, M. E. Fenstermacher, I. Joseph, A. W. Leonard, T. H. Osborne, G. D. Porter, M. J. Schaffer, P. B. Snyder, P. R. Thomas, J. G. Watkins, and W. P. West, *Nat. Phys.* **2**, 419–423 (2006).